[AMERICAN JOURNAL OF SCIENCE, VOL. 275, FEBRUARY, 1975, P. 143-162]

EXPERIMENTAL AND THERMODYNAMIC STUDY OF EQUILIBRIA IN THE SYSTEM $CaO–MgO–SiO_2–H_2O–CO_2$

J. SLAUGHTER*, D. M. KERRICK*, and V. J. WALL**

ABSTRACT. Experimental brackets have been obtained for several equilibria in the system $CaO–MgO–SiO_2–H_2O–CO_2$. Reactions investigated, with corresponding equilibrium conditions, are as follows: (1) 5 talc + 6 calcite + 4 quartz = 3 tremolite + 6 CO_2 + 2 H_2O (Pf = 2 kb, 440 ± 15°C, X_{CO_2} = 0.50); (2) tremolite + 3 calcite + 2 quartz = 5 diopside + 3 CO_2 + H_2O (Pf = 1 kb, 494 ± 10°C, X_{CO_2} = 0.50) (Pf = 1 kb, 486 ± 15°C, X_{CO_2} = 0.90) (Pf = 5 kb, 637 ± 5°C, X_{CO_2} = 0.85); (3) dolomite + 2 quartz = diopside + 2 CO_2 (Pf = 1 kb, 442 ± 15°C, X_{CO_2} = 0.95) (Pf = 2 kb, 515 ± 15°C, X_{CO_2} = 0.95); (4) tremolite + 3 calcite = dolomite + 4 diopside + H_2O + CO_2 (Pf = 5 kb, 649 ± 5°C, $X_{CO_2} > 0.82$); (5) 5 dolomite + 8 quartz + H_2O = tremolite + 3 calcite + 7 CO_2 (Pf = 2 kb, 484 ± 15°C, X_{CO_2} = 0.85). These data provide starting points for the thermodynamic calculation of phase equilibria in this system. Reaction direction was determined by (A) weight changes of single quartz spheres, (B) X-ray examination of all-powder runs, (C) quantitative analysis of the amount of calcite and/or dolomite formed or consumed. Using $\Delta G_{reaction}$ based on the above equilibrium data, free energy and activity data for CO_2 and H_2O, and published and estimated entropy and volume data for solid phases, self-consistent T-X topologies were calculated at 1 and 2 kb. These equilibria are compatible with the experimental data of Skippen (1971) but possess much lower uncertainties. The talc + calcite stability field is much less extensive at 1 kb than was indicated in the T-X topology of Metz and Trommsdorff (1968). Contrary to Skippen (1974) our calculations show that the talc + calcite stability field is of reduced extent with increasing pressure.

LIST OF SYMBOLS

a_{CO_2}, a_{H_2O} — activities of CO_2 and H_2O.

G_{CO_2}, G_{H_2O} — free energy of *pure* CO_2 and H_2O.

ΔG_r — free energy change of reaction.

n_1, n_2 — number of moles of H_2O and CO_2, respectively, in the balanced reaction.

R — gas constant.

ΔS_r — entropy change of reaction.

ΔS_s — entropy change for the solid phases in the balanced reaction

T — temperature in degrees Kelvin.

ΔV_s — volume change of the solid phases in the balanced reaction.

INTRODUCTION

Phase relations have been investigated in the $CaO–MgO–SiO_2–H_2O–CO_2$ system by several experimentalists, and T-X_{CO_2} topologies have been constructed by Skippen (1971) and by Metz and Trommsdorff (1968). Inconsistencies are evident between these published topologies.

* Department of Geosciences, The Pennsylvania State University, University Park, Pa. 16802

** Department of Earth Sciences, Monash University, Melbourne, Australia

The reactions investigated experimentally in this study are:

$$5 \text{ talc} + 6 \text{ calcite} + 4 \text{ quartz} = 3 \text{ tremolite} + 6\ CO_2 + 2\ H_2O \quad (1)$$

$$\text{tremolite} + 3 \text{ calcite} + 2 \text{ quartz} = 5 \text{ diopside} + 3\ CO_2 + H_2O \quad (2)$$

$$\text{dolomite} + 2 \text{ quartz} = \text{diopside} + 2\ CO_2 \quad (3)$$

$$\text{tremolite} + 3 \text{ calcite} = \text{dolomite} + 4 \text{ diopside} + CO_2 + H_2O \quad (4)$$

$$5 \text{ dolomite} + 8 \text{ quartz} + H_2O = \text{tremolite} + 3 \text{ calcite} + 7\ CO_2 \quad (5)$$

Determination of the locations of these reactions on isobaric T-X_{CO_2} diagrams establishes the locations of two key invariant points and, consequently, fixes the remaining equilibria intersecting in these invariant points. The phase equilibria of much of this chemical system are thereby determined, and physical conditions of various metamorphic parageneses are implied.

EXPERIMENTAL DETAILS

Experiments were conduced at 1, 2, and 5 kb. For equilibria involving quartz, reaction direction was monitored by weight changes of single quartz crystals. For reactions not involving quartz, runs with all-powdered starting mixtures were performed. Duration of runs was generally 21 days for the 1 and 2 kb experiments, although some 30-day runs were conducted with all-powdered charges. Duration of 5 kb runs was 18 days.

For single crystal runs, quartz spheres, weighing between 0.005 and 0.01 g, were prepared from a visually flawless specimen of Brazilian quartz. Each weight recorded for a quartz sphere was the average of five replicate weighings on a Mettler M-5 microbalance; individual weighings agreed to within 5 micrograms.

For all-powder runs, reaction direction was determined by comparing relative X-ray peak heights of phases in starting mixtures and run products. Where applicable, atomic absorption analysis of solutions prepared from run products as compared with those from starting mixtures was employed to determine changes in the quantity of carbonate phases during runs.

The desired fluid compositions were achieved by adding oxalic acid or a mixture of water and silver oxalate. Fluid composition was checked after runs by the method of Johannes (1969, p. 1085). Reproducibility in X_{CO_2} was $\pm$ 0.035 where silver oxalate and water were used together; with oxalic acid (used to produce $X_{CO_2} = 0.50$) fluid compositions were reproducible to $\pm$ 0.01.

For single crystal runs, individual quartz spheres were loaded into Pd-Ag capsules, along with 0.02 g of a powdered mixture of the addi-

tional solid phases in the reaction. The powder (< 325 mesh) is a mixture of equal weights of the requisite phases; ultra-fines were decanted from the mixture in aqueous suspension. For CO_2-rich fluid compositions, 0.03 g of Ag-oxalate was added, and the requisite quantity of water introduced. Capsules with X_{CO_2} of 0.50 initially contained 0.015 g of oxalic acid. For all-powder runs, 0.02 g of the appropriate powdered mixture was loaded, and the desired fluid composition was achieved as described for single crystal runs.

Runs at 1 and 2 kb were made with 1 inch O. D. René cold seal pressure vessels. For each vessel, temperatures were monitored with external chromel-alumel thermocouples and recorded on a multichannel recorder. Thermocouples were calibrated before and after runs by comparison with a standard thermocouple calibrated against the melting point of gold. Runs were terminated by cooling the bombs in a jet of compressed air.

Runs at 5 kb were performed in internally heated pressure vessels with an argon pressure medium.

SUMMARY OF EXPERIMENTAL DATA

Weight change diagrams obtained for reactions (1), (2), (3), and (5) are shown in figures 1 through 7. The uncertainty in each recorded weight change corresponds to the maximum deviation among five replicate weighings. The 10°C uncertainty in the location of data points shown on the weight change diagrams incorporates uncertainties from several sources, such as thermocouple drift, temperature fluctuation, et cetera.

TABLE 1

Chemical composition of starting materials*

	Tremolite	Diopside	Talc	Calcite	Dolomite
SiO_2	58.2	54.5	61.6	<0.1	<0.1
TiO_2	<0.02	<0.02	<0.02	<0.02	<0.02
Al_2O_3	0.07	<0.05	0.19	—	—
Fe_2O_3	0.30	—	0.1	<0.01	0.79
FeO	0.27	0.61	—	—	—
MnO	0.02	0.06	0.03	<0.005	.08
MgO	24.2	18.0	31.0	<0.05	21.19
CaO	14.8	25.6	0.41	56.30	30.99
Na_2O	<0.05	<0.05	<0.05	<0.05	<0.05
K_2O	<0.05	<0.05	<0.05	<0.05	<0.05
SrO	—	—	—	<0.35	<0.025
H_2O**	2.21	—	4.75	—	—
CO_2	—	—	—	43.70	46.90
F	0.07	—	0.33	—	—
Total	99.87	98.77	98.41	100.00	99.95

Chemical formulas

Tremolite: $Ca_{2.16}$ $(Mg_{4.91}$ $Fe_{0.03}{}^{+2})$ $(Si_{7.92}$ $Al_{0.01})$ O_{22} $(OH_{2.00}$ $F_{0.03})$

Diopside: $Ca_{1.00}$ $(Mg_{0.98}$ $Fe_{0.02}{}^{+2})$ $Si_{2.00}$ $O_{6.00}$

Talc: $Ca_{0.06}$ $(Mg_{5.97}$ $Fe_{0.01}{}^{+3})$ $(Si_{7.91}$ $Al_{0.03})$ O_{20} $(OH_{4.06}$ $F_{0.01})$

Calcite: $Ca_{1.00}$ $(CO_3)_{1.00}$

Dolomite: $Ca_{1.03}$ $(Mg_{0.98}$ $Fe_{0.02})$ $(CO_3)_{1.98}$

* Analyses by J. Bodkin, J. Slaughter, and N. Suhr.

** Calculated from ideal chemical formulas of tremolite and talc.

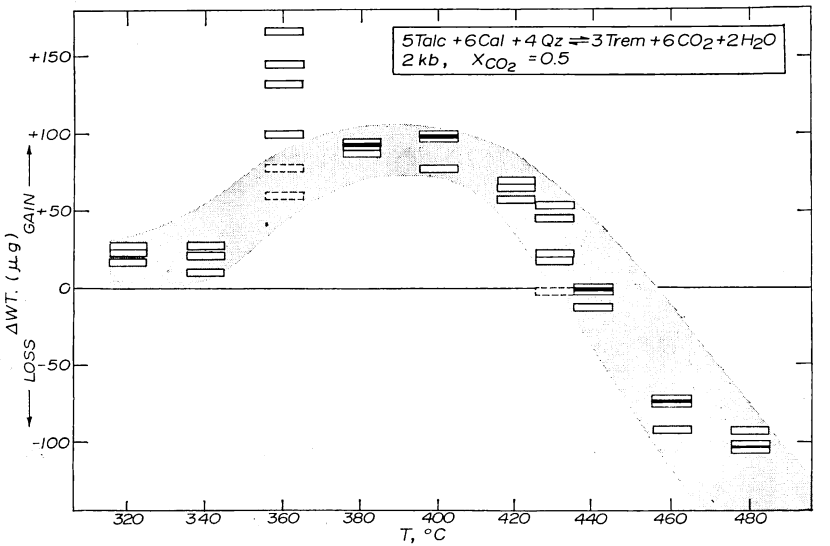

Fig. 1. Experimental results of single crystal runs on reaction (1) at Pf = 2 kb, X_{CO_2} = 0.50. Dashed rectangles are from "tremolite-free" capsules (see below). Duration of runs was 21 days. Vertical and horizontal dimensions of rectangles in this and subsequent weight change diagrams give the uncertainties in weight change and temperature, respectively, of individual data points. Overlap of rectangles is indicated by black bands.

Mineral abbreviations for figures: Cal = calcite; Diops = diopside; Dol = dolomite; Qz = quartz; Tr, Trem = tremolite; Fo = forsterite.

Equilibrium for a given reaction is taken as the temperature interval where a band fitted to the data points crosses the zero weight change line. As has been demonstrated in a recent study by Shettel (1973), corrections for the solubility of quartz in such CO_2-rich fluids are negligible. We have verified that the solubility correction is negligible in runs with capsules that contained only quartz spheres and a CO_2-rich fluid.

Experimental results of single crystal and of all-powder runs on reaction (1) at 2 kb are presented in figure 1 and table 2, respectively. The weight change diagram indicates that near 360°C there are anomalously large weight gains. This inflection indicates the occurrence of an accompanying reaction, which, from phase equilibrium considerations, could be:

$$3 \text{ dolomite} + 4 \text{ quartz} + H_2O = \text{talc} + 3 \text{ calcite} + 3\ CO_2$$

To gauge the extent of the secondary reaction, capsules were run that contained no tremolite but were otherwise identical in their contents to the other capsules used in the single crystal study of reaction (1). The data points corresponding to these capsules are shown as dashed rectangles in figure 1. Since, in the absence of tremolite, reaction (1) cannot operate, the weight gains obtained for the tremolite-free capsules run at 360°C reflect the extent of the secondary reaction. If the data

points at 360°C corresponding to capsules that contained the entire assemblage of reaction (1) are adjusted to account for the extent of the secondary reaction, they fall in line with the trend of the remaining data. Another tremolite-free capsule was run at the temperature of the zero reaction point (fig. 1). Virtually no weight change occurred in this run, such that no secondary reaction occurred at this temperature. All-powder runs on reaction (1) indicate equilibrium at the same temperature as inferred from single crystal runs: 440 ± 15°C at $X_{CO_2} = 0.50$ and 2 kb. The same equilibrium is indicated by monitoring changes in the amount of quartz and of calcite. Therefore, the zero reaction point represents equilibrium for one reaction and not the composite effect of more than one reaction.

Since data on the weight change diagram of figure 1 at temperatures between 360°C and the crossover do not exhibit the high degree of scatter possessed by the data points at 360°C, it is inferred that the secondary reaction does not operate above approximately 360°C. The data of figure 1 (after adjustment of the 360°C points for the extent of secondary reaction) exhibit a broad positive inflection at temperatures below the zero point. This inflection is compatible with the fact that reaction rate decreases at lower temperatures.

Figure 2 is a weight change diagram of quartz crystals for runs on reaction (2) at 1 kb and $X_{CO_2} = 0.50$. Equilibrium is inferred to be 494 ± 10°C. A positive effect of temperature on reaction kinetics is clearly indicated at temperatures above the zero reaction point. The positive inflection in the weight change curve at temperatures below the zero point, as for reaction (1), is compatible with the fact that reaction rate decreases at lower temperatures. Although the exact location of the weight change curve fitted to the data points is uncertain, it is important that above 495°C all crystals lost weight whereas at lower tempera-

TABLE 2

Results of 2 kb all-powder runs on reaction (1):
5 talc + 6 calcite + 4 quartz = 3 tremolite + 6 CO_2 + 2 H_2O

Capsule no.	X_{CO_2}	T °C of run	Wt % calcite in run product by atomic absorption*		Reaction direction
1a	0.50	420	27.70	28.30	Talc←
2a	0.50	420	28.00	28.40	Talc←
3a	0.50	420	28.15	28.15	Talc←
4a	0.50	440	27.50	28.00	N.R.
5a	0.50	440	26.50	27.00	N.R.
6a	0.50	440	27.50	28.00	N.R.
2	0.50	460	20.40	19.90	→Tremolite
3	0.50	460	23.40	21.70	→Tremolite
5	0.50	500	21.90	22.40	→Tremolite
6	0.50	500	24.00	23.10	→Tremolite
7	0.50	550	14.25	14.50	→Tremolite
8	0.50	550	8.80	8.50	→Tremolite
9	0.50	550	12.70	13.40	→Tremolite

* Starting mix had 26.64 ± 1.2 percent calcite based on six atomic absorption analyses.

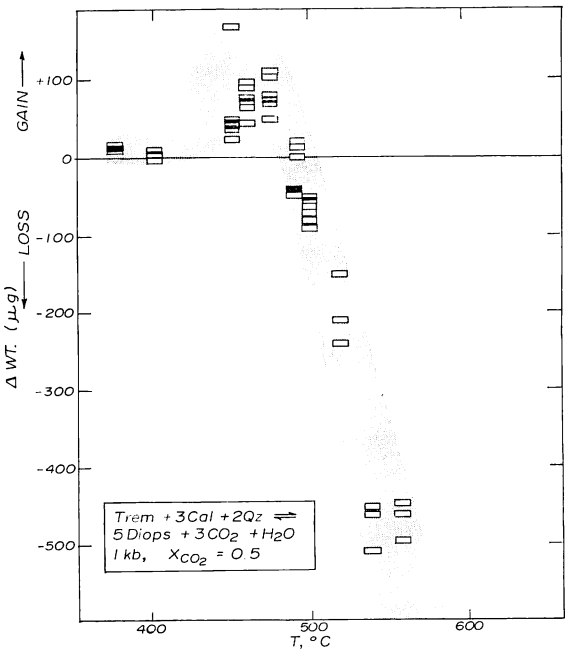

Fig. 2. Experimental results of single crystal runs on reaction (2) at Pf = 1 kb, X_{CO_2} = 0.50. Duration of runs was 21 days. Symbols as in figure 1.

tures weight gains were registered. Furthermore, significant weight gains were observed for runs at temperatures just below the crossover at 490°C. In addition, where reactions have been studied by all-powder methods (all-powder X-ray analysis or atomic absorption determination of change in proportion of carbonate phases present during runs), resulting experimental brackets are in accord with those obtained by the single crystal method (see the data of tables 2, 3, and 4). Consequently, it is concluded that reaction reversal has been demonstrated. Figure 3 is a weight change diagram for single crystal runs on reaction (2) at 1 kb and X_{CO_2} = 0.90. The experimental bracket at this fluid composition is taken as 486 ± 15°C.

Results of single crystal and of all-powder runs on reaction (2) at 5 kb are presented in tables 3 and 4 and in figure 4. The curve shown in figure 4 was calculated by extrapolation from a starting point of 639°C and X_{CO_2} = 0.80. This location of the curve separates data points for capsules that were in the stability field of diopside from those that showed reaction to the low temperature assemblage. It is evident that the location shown for reaction (2) achieves the best separation of data points of opposite reaction directions although there still remains one anomalous point (X_{CO_2} = 0.80, 649°C).

Determination of changes in proportions of carbonate phases by atomic absorption was applied ordinarily only to all-powder runs. At

given physical conditions, more reaction occurs in all-powder runs than in single crystal runs, and, for low pressure runs, the atomic absorption technique does not have sufficient sensitivity when applied to single crystal run products. However, reaction rate was sufficiently rapid at temperatures near the inferred equilibrium at 5 kb that the atomic absorption analysis for carbonates could be applied to both single crystal and all-powder run products. For individual capsules, there is agreement between direction of reaction inferred from single crystal data, X-ray studies, and atomic absorption analyses, indicating equilibrium for reaction (2) at 5 kb, 637 ± 5°C, at $X_{CO_2} = 0.85$.

TABLE 3

Results of 5 kb all-powder runs on reaction (2):
tremolite + 3 calcite + 2 quartz = 5 diopside + 3 CO_2 + H_2O

Powder no.	Temperature of run °C	X_{CO_2}	Average tremolite/diopside peak height ratio*	Reaction direction	Pairs of analyses for wt percent calcite by atomic absorption**	
C_1	627	0.50	0.910	→Diopside	24.60	24.60
C_2	638	0.50	1.506	→Diopside	21.90	22.20
C_3	649	0.50	0.622	→Diopside		
4	627	0.76	9.580	Tremolite←	35.65	36.00
5	638	0.76	6.620	Tremolite←	31.40	30.80
6	649	0.90	0.660	→Diopside	21.20	20.50
7	627	0.30	0.386	→Diopside	19.65	20.10
8	638	0.30	0.276	→Diopside		
9	649	0.30	0.0494	→Diopside	19.80	20.05

* Starting mix had an average tremolite/diopside peak height ratio of 4.78 with a standard deviation of 1.33 based on 5 scans.
** Starting mix had 27.1 ± 1.0 percent calcite based on six atomic absorption analyses.

TABLE 4

Results of single crystal runs on reaction (2) at 5 kb

Capsule no.	Temperature of run °C	X_{CO_2}	Wt change of quartz sphere	Reaction direction	Pairs of analyses for wt percent calcite by atomic absorption*	
7	649	0.36	−365	→Diopside		
8	638	0.37	−365	→Diopside	24.20	24.20
9	627	0.37	−326	→Diopside	26.80	26.90
10	649	0.51	−301	→Diopside	25.60	24.75
11	627	0.51	−274	→Diopside	24.00	24.10
12	638	0.51	−295	→Diopside	38.20	37.95
13	649	0.80	+32	Tremolite←		
14	627	0.81	+46	Tremolite←		
15	638	0.82	+34	Tremolite←		
16	635	0.66	−139	→Diopside	39.80	40.55
17	645	0.75	−175	→Diopside	40.20	41.15
18	655	0.75	−237	→Diopside	37.10	37.40
19	635	0.87	−30	→Diopside	41.45	42.10
20	645	0.87	−190	→Diopside	40.30	40.40
21	655	0.875	−162	→Diopside	39.50	39.50

* Starting mix for capsules 8 through 12 had 38.8 ± 1.5 wt percent calcite based on six atomic absorption analyses.
Starting mix for capsules 16 through 21 had 42.75 ± 1.5 wt percent calcite based on six atomic absorption analyses.

Figure 5 is a weight change diagram of single crystals for runs on reaction (3) at 1 kb and $X_{CO_2} = 0.95$. Equilibrium is inferred to be at 442 ± 15°C. Figure 6 gives single crystal data for runs on reaction (3) at 2 kb and $X_{CO_2} = 0.95$. Equilibrium at 2 kb is inferred to be at 515 ± 15°C and $X_{CO_2} = 0.95$.

The reproducibility of fluid composition in these CO_2-rich fluids has been stated as ± 0.035 in X_{CO_2}. Therefore, the fluid composition (X_{CO_2}) of capsules for reaction (3) varied from approximately 0.915 to 0.985. Earlier runs on reaction (3), in which a nearly H_2O-free silver oxalate had been used to generate CO_2, yielded no observable weight changes for crystals, indicating the dependence of finite reaction on the presence of H_2O.

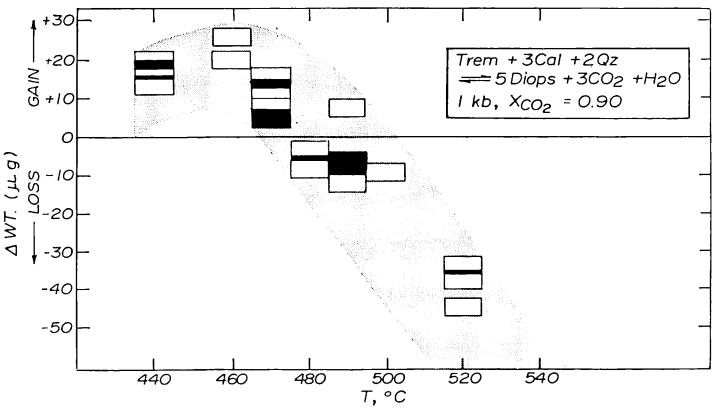

Fig. 3. Experimental results of single crystal runs on reaction (2) at Pf = 1 kb, $X_{CO_2} = 0.90$. Duration of runs was 21 days. Symbols as in figure 1.

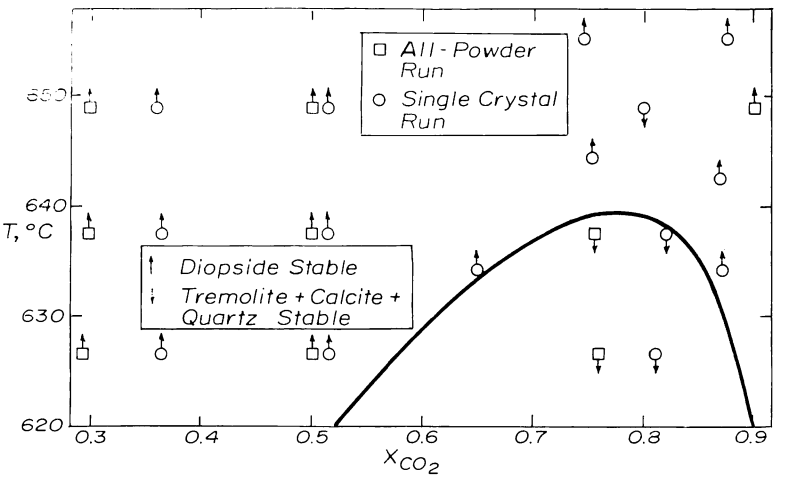

Fig. 4. Experimental results of all-powder and single crystal runs on reaction (2) at Pf = 5 kb. Duration of runs was 18 days.

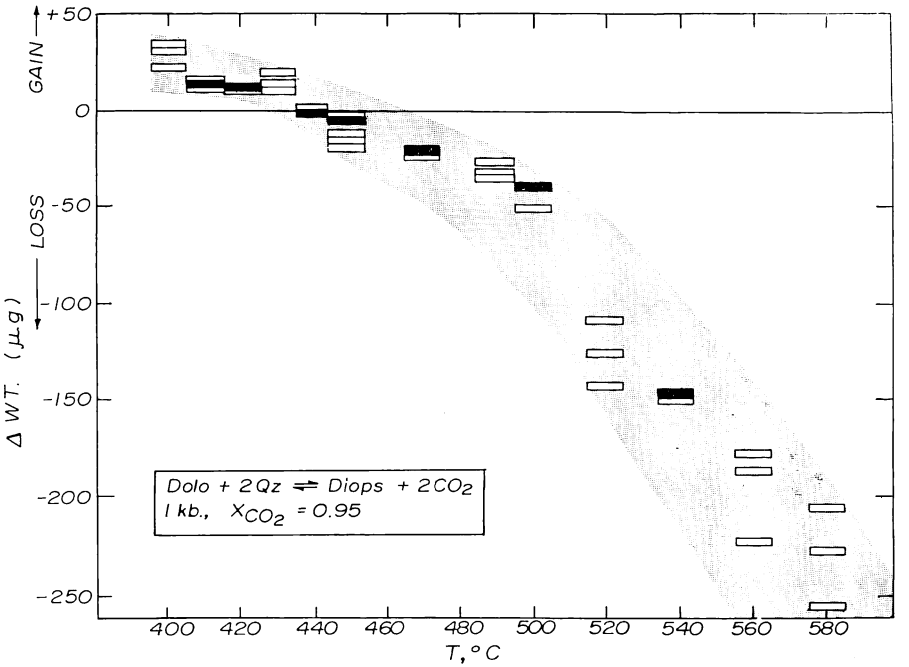

Fig. 5. Experimental results of single crystal runs on reaction (3) at Pf = 1 kb, $X_{CO_2} = 0.95$. Duration of runs was 21 days. Symbols as in figure 1.

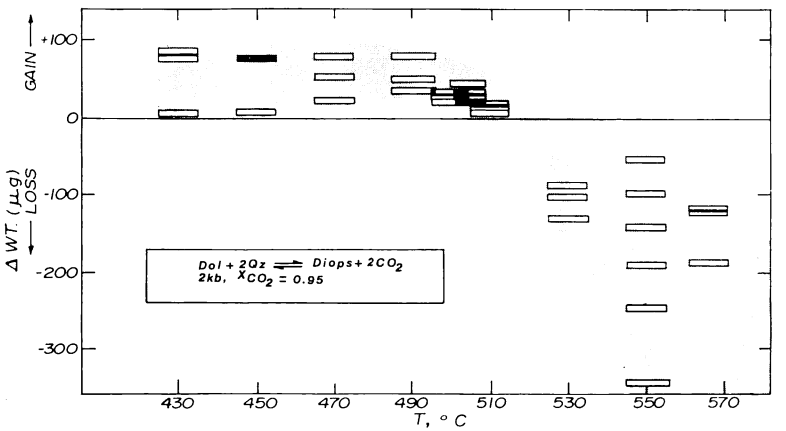

Fig. 6. Experimental results of single crystal runs on reaction (3) at Pf = 2 kb, $X_{CO_2} = 0.95$. Duration of runs was 21 days. Symbols as in figure 1.

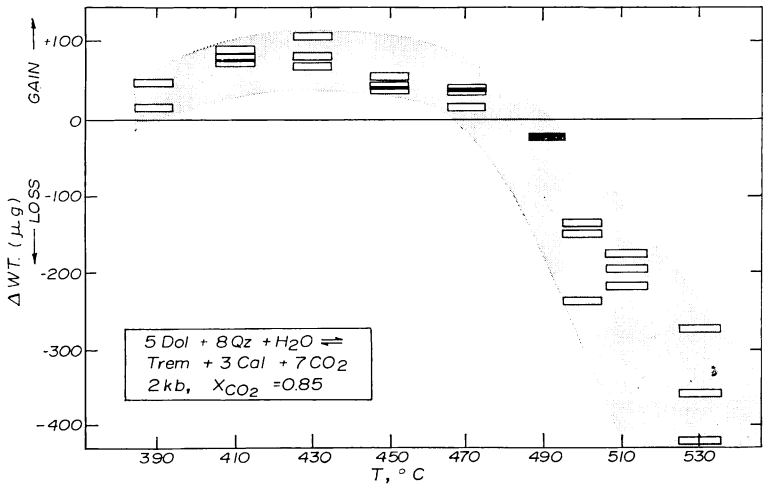

Fig. 7. Experimental results of single crystal runs on reaction (5) at Pf = 2 kb, $X_{CO_2} = 0.85$. Duration of runs was 21 days. Symbols as in figure 1.

The data for reaction (3) at 2 kb suggest that there is a dependence of reaction rate on water content. Table 5 shows that there is a general correlation of weight change with fluid composition for individual runs. The nonreproducibility of fluid composition coupled with the apparent relationship of reaction rate to fluid composition could account for the scatter noted in the weight change diagram for reaction (3) in figure 6. Runs of $X_{CO_2} = 0.50$ (generated with oxalic acid) are reproducible to $\pm$ 0.01 X_{CO_2} and, therefore, are likely to be less affected by the variation in reaction rate with fluid composition.

Results of all-powder runs at 5 kb on reaction (4) are given in table 6. Reaction direction as indicated by X-ray and atomic absorption analysis is in agreement for individual capsules. The equilibrium inferred for reaction (4) is 649 $\pm$ 5°C, $X_{CO_2} > 0.82$ at 5 kb.

Results of single crystal runs on reaction (5) at 2 kb are presented in figure 7, suggesting equilibrium at 484 $\pm$ 15°C, $X_{CO_2} = 0.85$.

THERMODYNAMIC CALCULATIONS AND CONSTRUCTION OF T-X TOPOLOGIES

The following expression permits determination of the free energy change of a reaction at new P, T, and X values if an initial equilibrium point is known ($\Delta G_r = 0$).

$$\Delta\Delta G_r = \int_{P_1}^{P_2} \Delta V_s dP - \int_{T_1}^{T_2} \Delta S_s dT + n_1 [(G_{H_2O})_{P_2, T_2} - (G_{H_2O})_{P_1, T_1}]$$
$$+ n_1 [RT_2 \ln(a_{H_2O})_{P_2, T_2} - RT_1 \ln(a_{H_2O})_{P_1, T_1}]$$
$$+ n_2 [(G_{CO_2})_{P_2, T_2} - (G_{CO_2})_{P_1, T_1}]$$
$$+ n_2 [RT_2 \ln(a_{CO_2})_{P_2, T_2} - RT_1 \ln(a_{CO_2})_{P_1, T_1}] \quad (1)$$

Here ΔS_s, the entropy change for the solid phases, is an analytical function of T. Power series expressions for entropies as a function of temperature were obtained by fitting third law entropies reported by Robie and Waldbaum (1968) to an expression of the form $S_T = A(\ln T) + BT + CT^{-2} + D$. Free energies of water were taken from Burnham, Holloway, and Davis (1969), and free energies for CO_2 are from unpublished data of Burnham and Wall. The standard state for the volatiles is 298.15°K and 1 bar. The differential compressibility of solid phases is of negligible consequence for these reactions and was not considered.

For isobaric equilibrium we have:

$$\begin{aligned} 0 = \Delta\Delta G_r = &- \int_{T_1}^{T_2} \Delta S_s dT + n_1 [(G_{H_2O})_{P_1, T_2} - (G_{H_2O})_{P_1, T_1}] \\ &+ n_1 [RT_2 \ln(a_{H_2O})_{P_1, T_2} - RT_1 \ln(a_{H_2O})_{P_1, T_1}] \\ &+ n_2 [(G_{CO_2})_{P_1, T_2} - (G_{CO_2})_{P_1, T_1}] \\ &+ n_2 [RT_2 \ln(a_{CO_2})_{P_1, T_2} - RT_1 \ln(a_{CO_2})_{P_1, T_1}] \end{aligned} \quad (2)$$

The isobaric free energy change of a pure volatile species (v) is:

$$(G_v)_{P_1, T_2} - (G_v)_{P_1, T_1} = - \int_{T_1}^{T_2} S_v dT$$

Substitution of such an integral for the free energy changes of pure H_2O and CO_2 in equation (2) results in:

$$\begin{aligned} 0 = &- \int_{T_1}^{T_2} \Delta S_s dT - \int_{T_1}^{T_2} (S_{H_2O}) dT - \int_{T_1}^{T_2} (S_{CO_2}) dT \\ &+ n_1 [RT_2 \ln(a_{H_2O})_{P_1, T_2} - RT_1 \ln(a_{H_2O})_{P_1, T_1}] \\ &+ n_2 [RT_2 \ln(a_{CO_2})_{P_1, T_2} - RT_1 \ln(a_{CO_2})_{P_1, T_1}] \end{aligned}$$

which becomes:

$$\int_{T^1}^{T_2} \Delta S_r dT = RT_2 \ln[(a_{H_2O})^{n_1}(a_{CO_2})^{n_2}]_{T_2} - RT_1 \ln[(a_{H_2O})^{n_1}(a_{CO_2})^{n_2}]_{T_1} \quad (3)$$

Activity coefficients of H_2O and CO_2 have been obtained by interpolation and extrapolation of the data in the tables of Rhyzhenko and Malinin (1971). Since $a = \gamma x$, activities can then be obtained by the product of activity coefficient and corresponding mole fraction. A table of activities for both CO_2 and H_2O as a function of X_{CO_2} and T was obtained at 1 and 2 kb. This permits determination of the activities of H_2O and CO_2 in equation (3) and, finally, determination of the equilibrium X_{CO_2} for any temperature (T_2) chosen in equation (3).

TABLE 5

Relationship of wt change of crystals to X_{H_2O} for reaction (3) at 2 kb

Run no.	T °C of run	X_{H_2O} in capsule	Change in wt of crystal (μg)
1	447	0.04	+9
"	"	0.07	+80
"	"	0.08	+79
2	466	0.04	+17
"	"	0.06	+24
"	"	0.08	+80
3	485	0.05	+35
"	"	0.06	+51
"	"	0.07	+81
4	505	0.06	+10
"	"	0.07	+19
"	"	0.09	+19
5	528	0.05	−85
"	"	0.06	−102
"	"	0.07	−130
6	545	0.03	−142
"	"	0.07	−245
"	"	0.08	−345
7	423	0.07	+78
"	"	0.07	+88
"	"	0.05	+5
8	497	0.05	+24
"	"	0.06	+34
"	"	0.05	+27
9	502	0.04	+27
"	"	0.06	+43
"	"	0.05	+32
10	546	0.04	−99
"	"	0.01	−99
"	"	0.03	−54
11	565	0.04	−181
"	"	0.04	−117
"	"	0.03	−120

TABLE 6

Results of 5 kb all-powder runs on reaction (4): tremolite + 3 calcite = dolomite + 4 diopside + CO_2 + H_2O

Powder no.	Temperature °C of run	X_{CO_2}	Average tremolite/dolomite peak height ratio*	Reaction direction	Wt percent calcite (first column) and dolomite by atomic absorption**	
10	627	0.49	2.170	Tremolite←	44.50	18.60
11	649	0.50	8.015	Tremolite←	38.50	19.15
12	627	0.62	1.528	Tremolite←	34.40	21.70
13	649	0.63	1.159	Tremolite←	36.50	20.05
14	627	0.80	1.422	Tremolite←	37.02	20.60
15	649	0.82	1.642	Tremolite←	32.60	22.45

* Starting mix had an average tremolite/dolomite peak height ratio of 0.536 with a standard deviation of 0.131 based on 5 scans.

** Starting mix had 25.4 ± 1.0 wt percent dolomite and 30.6 ± 1.3 percent calcite based on six atomic absorption analyses.

Using equation (3) and the end points of experimental brackets, curves were obtained that set both the upper and lower limits of a region of uncertainty wherein the univariant curve can lie. These curves are extrapolated to locate invariant points and, consequently, to provide starting points for calculations of other curves that were not experimentally investigated.

Graphical location of intersections of extrapolated curves to provide starting points on derived equilibria can be quite inexact. However, a method of coupling free energy changes of reaction can be used instead to locate derived equilibria. If two reactions or multiples of those reactions are added to yield a third reaction, then the ΔG_r values (or their appropriate multiples) at the same P, T, and X_{CO_2} can be added to yield the ΔG_r of the third reaction. The ΔG_r values for reactions to be coupled[1] can be determined at any convenient P, T, and X_{CO_2} by equation (1) if they are known at some initial P, T, and X_{CO_2}. Since the reactions used for coupling have upper and lower limits of uncertainty, the ΔG_r values calculated for them at any P, T, and X_{CO_2} from equation (1) will have maximum and minimum values depending upon which of the two uncertainty limits provided the starting point of calculation. Therefore, the ΔG_r of the reaction derived by coupling will have a maximum and minimum value at a given P, T, and X_{CO_2}. Limits on the location of the coupled reaction are then obtained by determining where ΔG_r goes to zero with varying P, T, and X_{CO_2} according to equation (1). This method of coupling free energy terms will also couple the uncertainties in the ΔG_r values. Consequently, the locations of coupled reactions commonly have more uncertainty than is the case for experimentally located curves.

By the methods of calculation described above, T-X topologies have been calculated at 1, 2, and 5 kb. These are presented in figures 8 through 10. Since activity data are not available above 2 kb, the 5 kb topology was constructed on the assumption of ideal mixing in the fluid phase.

The locations of univariant curves on the T-X diagrams have been chosen within their limits of uncertainty according to the following criteria: (1) mutual intersection of the curves entering invariant points will be exactly achieved, and (2) the locations of individual curves portrayed in the 1 and 2 kb topologies will be consistent with extrapolations between these pressures, considering only uncertainties in thermodynamic quantities involved in the extrapolations. Therefore, the 1 and 2 kb topologies are internally consistent and consistent with each other.

The fact that experimental brackets have been obtained on some reactions at more than one pressure or X_{CO_2} value provides an opportunity to evaluate the compatibility of the experiments. It should be noted that uncertainties in the experimental brackets are far smaller than those that apply to the direct calculation of these equilibria using

[1] A "coupled reaction" is defined as one that has been derived by the appropriate addition of two other equilibria.

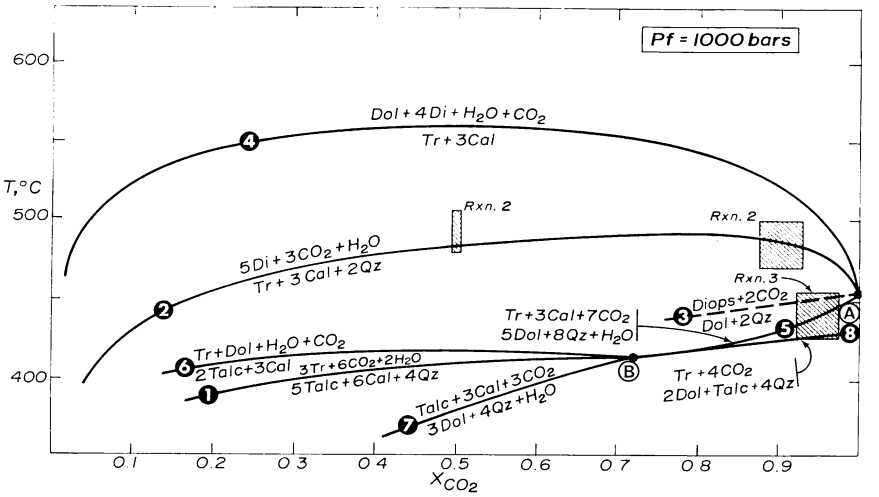

Fig. 8. T-X topology at Pf = 1 kb illustrating all reactions entering invariant points A and B; constructed through thermodynamic extrapolations from experimentally located points, with correction for nonideality of the fluid phase. The locations and uncertainties of experimental brackets are shown (hachured area).

the thermodynamic data of Robie and Waldbaum (1968) and free energy or fugacity data for H_2O and CO_2. Consequently, the experimental results can be used to make refinements in the thermodynamic data.

As shown in figure 11a, T-X extrapolations of the two experimental brackets on reaction (2) at 1 kb are in good agreement. A recalculation of our experimental bracket of reaction (2) at 5 kb to 1 kb is also shown. The 5 kb experimental bracket of reaction (2), appearing in figure 11a, has a large uncertainty in X_{CO_2}, since runs were performed at several fluid compositions, and the selected equilibrium bracket involves data points of differing fluid compositions (see fig. 4). The thermal uncertainty of the 5 kb experiments, however, is only ±5°C.

Where two experimental brackets are available at different pressures or, isobarically, at different X_{CO_2} values, they can be used to refine that thermodynamic quantity regarded to be most uncertain in thermodynamic extrapolations between the experimental brackets. This approach necessitates the assumption, however, that the experimental brackets are completely valid and that one thermodynamic quantity is regarded as the main source of error. Such a test may be illustrated in figure 11b, where the incompatibility of the experimental bracket at 2 kb with that extrapolated from 1 kb could reflect error in the high temperature entropy of dolomite, which was derived from an extrapolated heat capacity function based on low temperature (≤300°K) measurements.

Additional evaluation of compatibility of the experiments is provided where more than two experimentally located curves intersect in an invariant point. This is the case for both invariant points A and B.

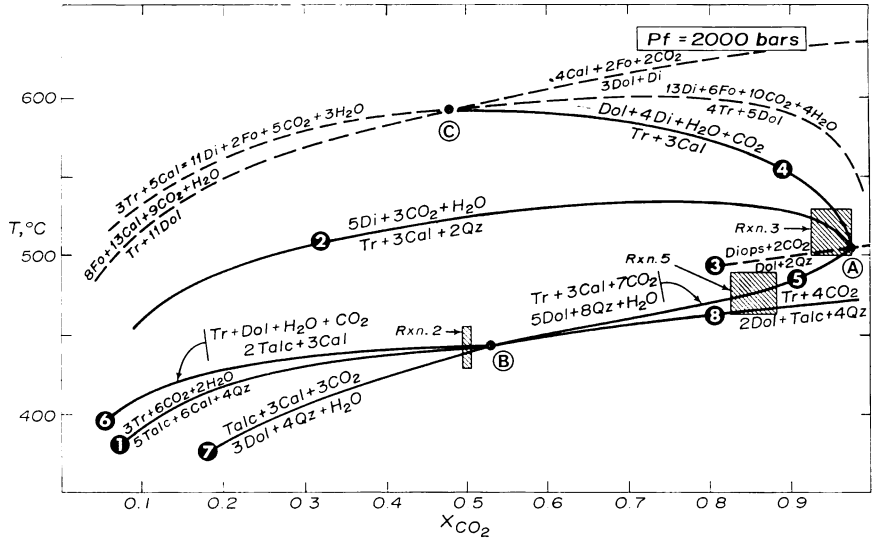

Fig. 9. T-X topology at Pf = 2 kb illustrating all reactions entering invariant points A and B; constructed through thermodynamic extrapolations from experimentally located points, with correction for nonideality of the fluid phase. The locations and uncertainties of experimental brackets are shown (hachured area). Dashed lines are the *schematic* illustration of equilibria involving forsterite.

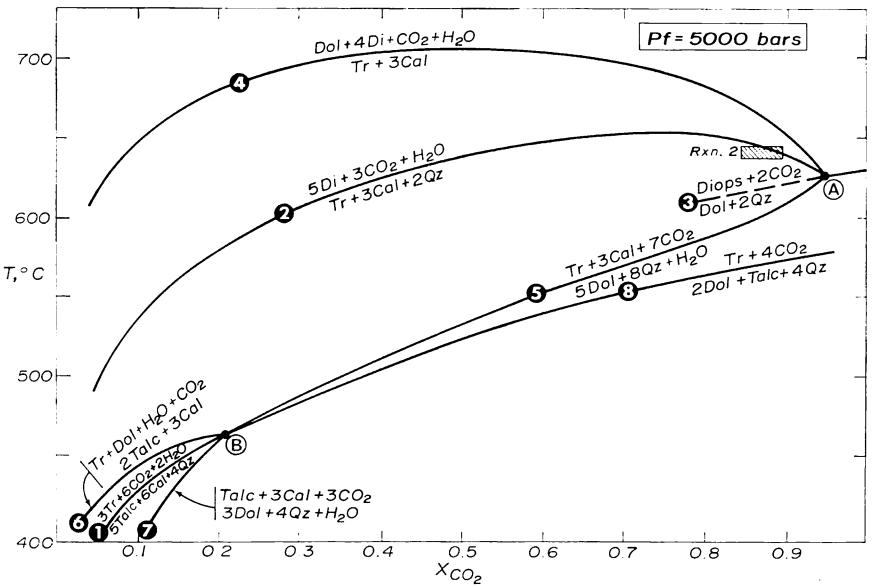

Fig. 10. T-X topology at Pf = 5 kb illustrating all reactions entering invariant points A and B; constructed through thermodynamic extrapolations from experimentally located points. The locations and uncertainty of the experimental bracket is shown (hachured area).

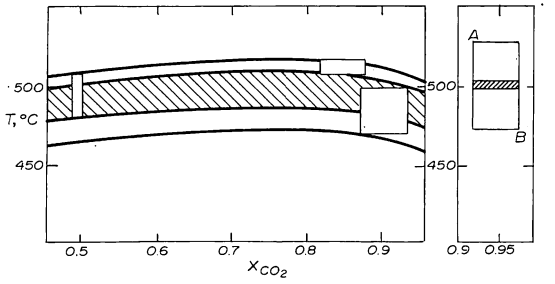

a. b.

Fig. 11. (a) Comparison of three experimental brackets on reaction (2) (open rectangles) at Pf = 1 kb. The experimental bracket at X_{CO_2} = 0.85 was recalculated to 1 kb from the 5 kb experimental results. The remaining two brackets were obtained at 1 kb. The curves shown are the activity-corrected extrapolations of the end points of the 1 kb brackets. The hachured area is the region of overlap between the two zones of uncertainty obtained by extrapolating the end points of the 1 kb brackets. (b) Comparison of two experimental brackets on reaction (3) at X_{CO_2} = 0.95 and Pf = 2 kb. A is the experimental bracket obtained at 2 kb, and B is a recalculation of the 1 kb bracket to 2 kb. The overlap of these brackets is indicated by hachuring.

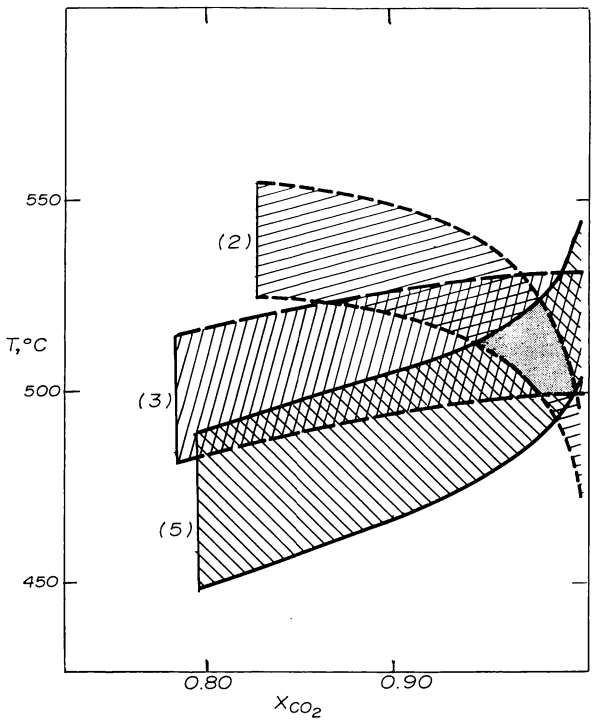

Fig. 12. Location of invariant point A based on the mutual intersection of reactions and their associated uncertainties. Pairs of curves shown for each reaction are the upper and lower limits of uncertainty wherein each curve must lie. Extrapolation of equilibria is discussed in the text. Area of mutual overlap is indicated by shading.

The degree of agreement between the mutual intersection of curves entering an invariant point is indicative of the compatibility of experimental results. This is illustrated for invariant point A at 2 kb in figure 12. The reactions are shown as bands whose widths correspond to the uncertainties in locations of reactions. The limits shown for each reaction were obtained by T-X extrapolations of end points of experimental brackets. Reaction (2) has been recalculated from the 1 kb experimental results. Reactions (3) and (5) have been calculated by T-X extrapolations from the 2 kb experimental brackets. The individual pairs of reactions intersect in curvilinear polygonal areas. The degree to which these areas overlap is indicative of the compatibility of the individual experimental studies. The mutual area of overlap provides an estimate of the location of reaction (4) which also intersects at this invariant point.

A similar diagram is provided for invariant point B in figure 13. Location of the reaction setting the lower limit of the talc + calcite stability field is taken from the data of Gordon and Greenwood (1970). The locations of reactions (1) and (5) are based on extrapolations from the 2 kb experiment brackets. Since the reactions entering invariant point B intersect at very small angles, location of the invariant point will be particularly sensitive to minor changes in slope or location of the equilibria. Therefore, consideration of nonideality in the calculation of these equilibria is of particular importance. In view of the angular relationship between these equilibria, the areas formed by the intersection of reactions and their associated uncertainties are elongated in the X_{CO_2} dimension.

In view of the fact that calcite and dolomite used in these experiments are close to end-member composition (table 1), equilibrium brackets for reactions (1), (2), and (3), which involve one carbonate phase,

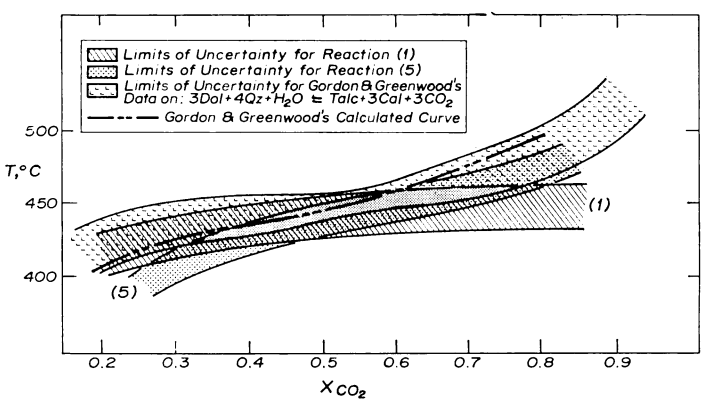

Fig. 13. Location of invariant point B at 2 kb based on the mutual intersection of reactions and their associated uncertainties. Pairs of curves shown for each reaction are the upper and lower limits of uncertainty wherein each curve must lie. Extrapolation of equilibria is discussed in the text. Area of mutual overlap is indicated by shading.

are uncomplicated by solid solution effects. Skippen's (1974) analysis suggests that solid solution changes in carbonate phases, related to the calcite–dolomite solvus, have a relatively unimportant effect on displacement of equilibria such as reactions (4) and (5), which involve both calcite and dolomite.

COMPARISON WITH PREVIOUSLY PUBLISHED EXPERIMENTAL RESULTS AND TOPOLOGIES

Metz (1970) performed experiments on reaction (2) and calculated the location of reaction (3). He derived the equilibrium constant for the given reaction from the free energy change of reaction at T and 1 bar, adjusted the equilibrium constant for pressure, and then determined the fugacities and corresponding mole fractions that satisfied the equilibrium constant at P and T. From his data on reactions (2) and (3), Metz inferred the location of invariant point A and, consequently, established other equilibria entering the invariant point. However, calculation of these equilibria from thermodynamic data alone is subject to considerable uncertainty. Furthermore, as shown in figure 14, the equilibrium temperatures claimed for reaction (2) by Metz are high in comparison with those of the present study and with Skippen's (1971) data. This *may* be attributed to inadequate demonstration of reaction reversibility on the part of Metz. His proof of reversibility is based on demonstrating that, once the fluid composition has changed toward the equilibrium composition at a given temperature, the fluid composition changes in the opposite direction in a subsequent run at lower temperature. However, since Metz does not reveal the magnitude of the temperature decrease in this experimental circuit, it is difficult to judge whether the fluid

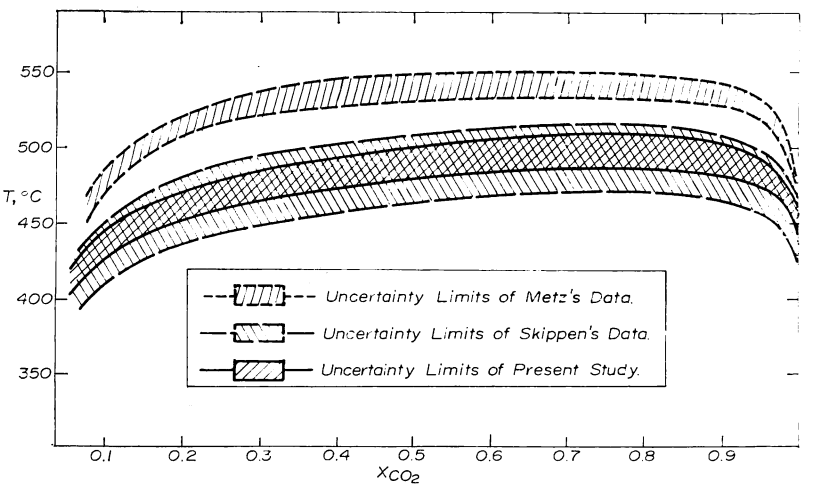

Fig. 14. Comparison of the results of the present study with those of Skippen (1971) and Metz (1970) on reaction (2) at Pf = 1 kb. Skippen's 2 kb experimental bracket has been recalculated to 1 kb and extrapolated in T-X space.

actually underwent a compositional reversal of measurable significance. The fact that reversibility was achieved would be less equivocal if the experimental circuit involved a large temperature decrease leading to a substantial reversal of the fluid composition.

Skippen (1971) determined experimentally the locations of five equilibria in the system $CaO–MgO–SiO_2–H_2O–CO_2$ and obtained equations relating log K to P and T for these five equilibria. These basic equations were then coupled to yield equations for other equilibria. However, since the uncertainties in the basic equations are compounded by this coupling, equations for derived equilibria have increased uncertainties. With Skippen's data, it is apparent that any estimate of the location of invariant points would be subject to very large uncertainties (Skippen, 1974), resulting in a large uncertainty in the topology.

Metz and Trommsdorff's (1968) topology shows both invariant points A and B at very CO_2-rich fluid compositions at 1 kb. Reaction (6): 2 talc + 3 calcite = tremolite + dolomite + H_2O + CO_2, which enters invariant point B, has a temperature maximum at $X_{CO_2} = 0.50$. Since this reaction sets the upper limit of the talc + calcite stability field, a large talc + calcite stability field results in Metz and Trommsdorff's topology, as demanded by their CO_2-rich location of invariant point B. Furthermore, since the aforementioned reaction intersects the equilibrium: tremolite + 11 dolomite = 8 forsterite + 13 calcite + 9 CO_2 + H_2O, another invariant point and other talc equilibria are generated. These features are inconsistent with the phase equilibria constructed on the basis of our experiments.

Equilibria involving forsterite are *schematically* show in figure 9. The reader is referred to Skippen (1971, 1974) for a more detailed discussion of the forsterite equilibria. It should be noted, however, that the T-X locations of the forsterite equilibria are subject to profound uncertainties. For example, our calculation of reaction (27) of Skippen (1971, 1974) shows a minimum temperature error (at $X_{CO_2} = 1.0$) of about ±40°C. Direct experimental investigation of these equilibria are clearly warranted.

Skippen's topology (1971) indicates a location and extent of the talc + calcite stability field at 2 kb that is compatible with that derived in the present study, although the uncertainty of his estimate is considerable. Skippen's recent contention (1974) that the talc + calcite stability field expands with increasing pressure is not corroborated by our calculations. Using equation (1), extrapolation of the reactions setting the upper and lower thermal limits of the talc + calcite stability field indicate that it is of reduced extent with increasing pressure, as is illustrated in progressing from figures 8 through 10. The relatively large stability field of talc + calcite at low pressures is compatible with the occurrence of this assemblage in some low-pressure contact aureoles (Tilley, 1948; Cooper, 1957). The restricted stability field of this assemblage at 5 kb is incompatible with the talc + calcite association in relatively high-pressure parageneses described by Trommsdorff (1972) and

by Puhan and Hoffer (1973). In contrast, from geothermometry obtained by application of the calcite–dolomite solvus, the assemblage talc + calcite must have a very restricted T-X_{CO_2} field in Grenville marbles metamorphosed at P = 4 to 5 kb (Hutcheon and Moore, 1973; Sobol and Essene, 1973). As pointed out by Skippen (1974) the high proportion of F in talc and tremolite from the Swiss Alps would be a complicating factor in the application of experimental data to natural parageneses.

ACKNOWLEDGMENTS

This study represents part of J. Slaughter's Ph.D. research at The Pennsylvania State University. We are grateful to George Skippen for his critical review of this paper. This research was supported by N.S.F. Grant GA-25685 to D. M. Kerrick.

REFERENCES

Burnham, C. Wayne, Holloway, J. R., and Davis, N. F., 1969, Thermodynamic properties of water to 1000°C and 10,000 bars: Geol. Soc. America Spec. Paper 132, 96 p.

Cooper, J. R., 1957, Metamorphism and volume losses in carbonate rocks near Johnson Camp, Cochise County, Arizona: Geol. Soc. America Bull., v. 68, p. 577-610.

Gordon, T. M., and Greenwood, H. J., 1970, The reaction: dolomite + quartz + water = talc + calcite + carbon dioxide: Am. Jour. Sci., v. 268, p. 225-242.

Hutcheon, I., and Moore, J. M., 1973, The tremolite isograd near Marble Lake, Ontario: Canadian Jour. Earth Sci., v. 10, p. 936-947.

Johannes, Wilhelm, 1969, An experimental investigation of the system MgO–SiO_2–H_2O–CO_2: Am. Jour. Sci., v. 267, p. 1083-1104.

Metz, P., 1970, Experimentelle untersuchung der metamorphose von kieselig dolomitishen sedimenten: Contr. Mineralogy Petrology, v. 28, p. 221-250.

Metz, P., and Trommsdorff, V., 1968, On phase equilibria in metamorphosed siliceous dolomites: Contr. Mineralogy Petrology, v. 18, p. 305-309.

Puhan, D., and Hoffer, E., 1973, Phase relations of talc and tremolite in metamorphic calcite-dolomite sediments in the southern portion of the Damara Belt (South West Africa): Contr. Mineralogy Petrology, v. 40, p. 207-214.

Robie, R. A., and Waldbaum, D. R., 1968, Thermodynamic properties of minerals and related substances at 298.15°K (25.0°C) and one atmosphere (1.013 bars) pressure and at higher temperatures: U.S. Geol. Survey Bull. 1259, 256 p.

Ryzhenko, B. N., and Malinin, S. D., 1971, The fugacity rule for the systems CO_2–H_2O, CO_2–CH_4, CO_2–N_2 and CO_2–H_2: Geochemistry Internat., p. 562-574.

Shettel, D. L., Jr., 1973, Solubility of quartz in H_2O-CO_2 fluids at 5 kb and 500°-900°C [abs.]: Am. Geophys. Union Trans., v. 54, p. 480.

Skippen, G. B., 1971, Experimental data for reactions in siliceous marbles: Jour. Geology, v. 79, p. 457-481.

———— 1974, An experimental model for low pressure metamorphism of siliceous dolomitic marble, Am. Jour. Sci., v. 274, p. 487-509.

Sobol, J. W., and Essene, E. J., 1973, Petrology of Grenville marbles from southern Ontario: Annual mtg. Geol. Soc. America Abs., p. 815.

Tilley, C. E., 1948, Earlier stages in the metamorphism of siliceous dolomites: Mineralog. Mag., v. 28, p. 272-276.

Trommsdorff, Volkmar, 1972, Change in T-X during metamorphism of siliceous dolomitic rocks of the Central Alps: Schweizer min. pet. Mitt., v. 52, p. 567-571.